Cell Reports, Volume *41*

Supplemental information

Inhibition of glutaminolysis restores mitochondrial function in senescent stem cells

Debanik Choudhury, Na Rong, Izuagie Ikhapoh, Nika Rajabian, Georgios Tseropoulos, Yulun Wu, Pihu Mehrotra, Ramkumar Thiyagarajan, Aref Shahini, Kenneth L. Seldeen, Bruce R. Troen, Pedro Lei, and Stelios T. Andreadis

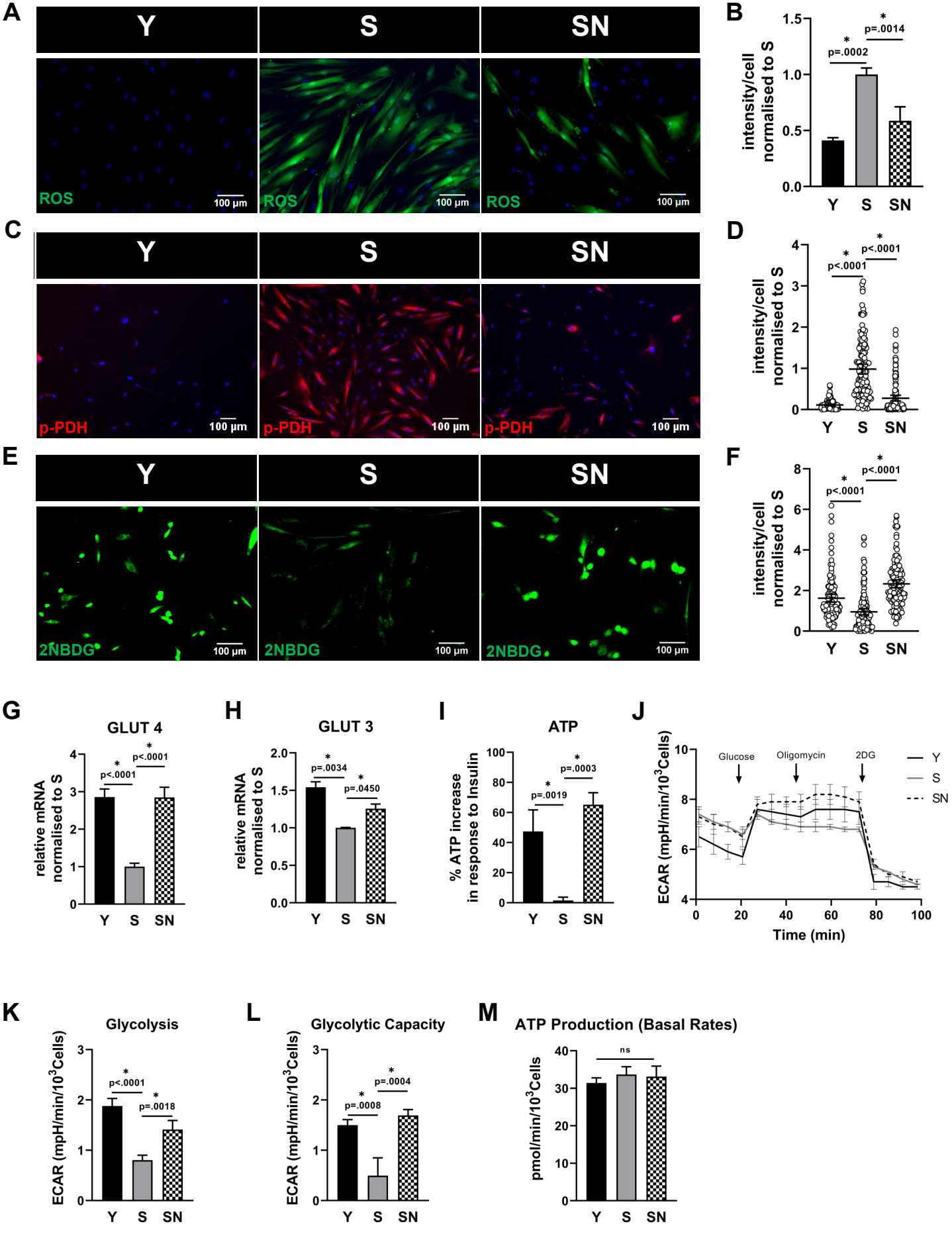
A
Y
S
SN
ROS
100 µm
B
intensity/cell normalised to S
p=.0002
p=.0014
Y S SN
C
p-PDH
D
p<.0001
E
2NBDG
F
G
GLUT 4
relative mRNA normalised to S
H
GLUT 3
I
ATP
% ATP increase in response to Insulin
p=.0019
p=.0003
J
Glucose
Oligomycin
2DG
ECAR (mpH/min/10³Cells)
Time (min)
K
Glycolysis
p=.0018
L
Glycolytic Capacity
p=.0008
p=.0004
M
ATP Production (Basal Rates)
pmol/min/10³Cells
ns

Figure S1. Senescent MSCs demonstrate reduced glycolysis. Related to Figure 1.

(A-B) Live stain images of reactive oxygen species (ROS) and quantification in Y, S and SN cells, using DCFDA dye; data shown as mean ± SD. (C) Immunostaining for p-PDH; scale bar=100μm. (D) Quantification of p-PDH intensity per cell, normalised to S; data shown as mean ± 95%CI for >100 cells. (E) Live stain images of 2-NBDG uptake, a fluorescent glucose analog; scale bar=100 μm. (F) Quantification of 2-NBDG intensity per cell, normalised to S; data shown as mean ± 95%CI for >100 cells. (G-H) Quantification of gene expression of glucose transporters, *GLUT4* and *GLUT3* via quantitative PCR normalised to S and internally normalised to *RPL32* cycle number; data shown as mean ± SD. (I) Intracellular ATP concentration measured after treatment with 100nM insulin for 24 hours; data represented as percentage increase in ATP concentration in response to insulin, shown as mean ± SD. (J-L) Measurement of extracellular acidification rate (ECAR) using seahorse analyzer and calculations of glycolysis and glycolytic capacity from glucose administration based ECAR data, demonstrating reduced glycolysis in senescent MSCs. (M) ATP production rate in Y, S, SN cells from ATP rate assay using seahorse flux analyzer. ns denotes not significant.

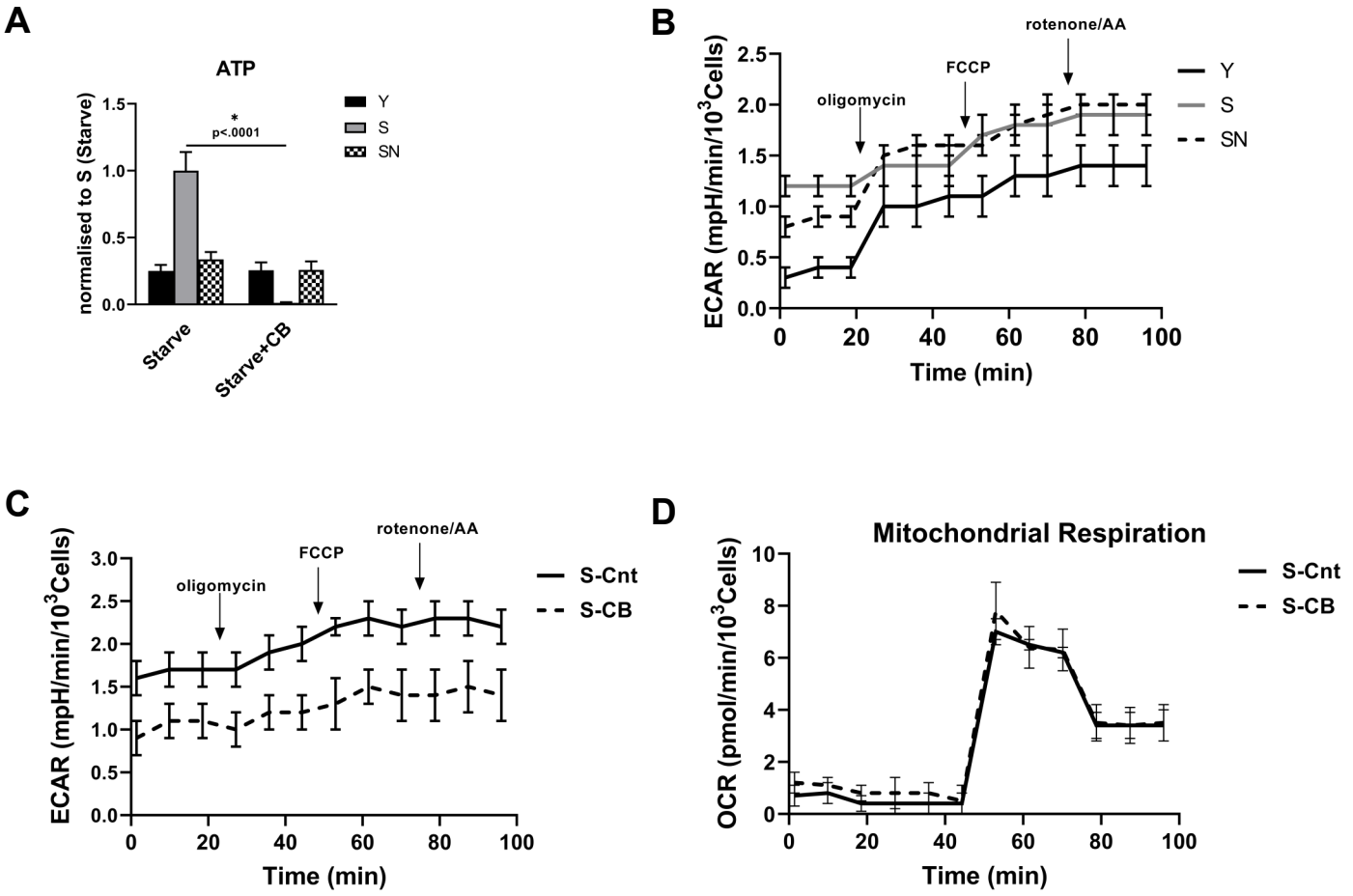

Figure S2. Blockade of GLS activity decreases ATP in senescent MSCs. Related to Figure 2.

(A) Intracellular ATP concentration measurement after starving Y, S and SN cells, without or without CB-839 (4μM) for 24hrs; data shown as mean ± SD. (B) Measurement of Extracellular Acidification Rate (ECAR) using seahorse analyzer after sequential addition of oligomycin, FCCP and rotenone/AA. (C) Measurement of ECAR in S cells after 24hours of treatment with CB-839 (4μM).(D) Measurement of oxygen consumption (OCR) using Seahorse extracellular flux analyzer in S cells after 24hrs treatment with CB-839 (4μM).

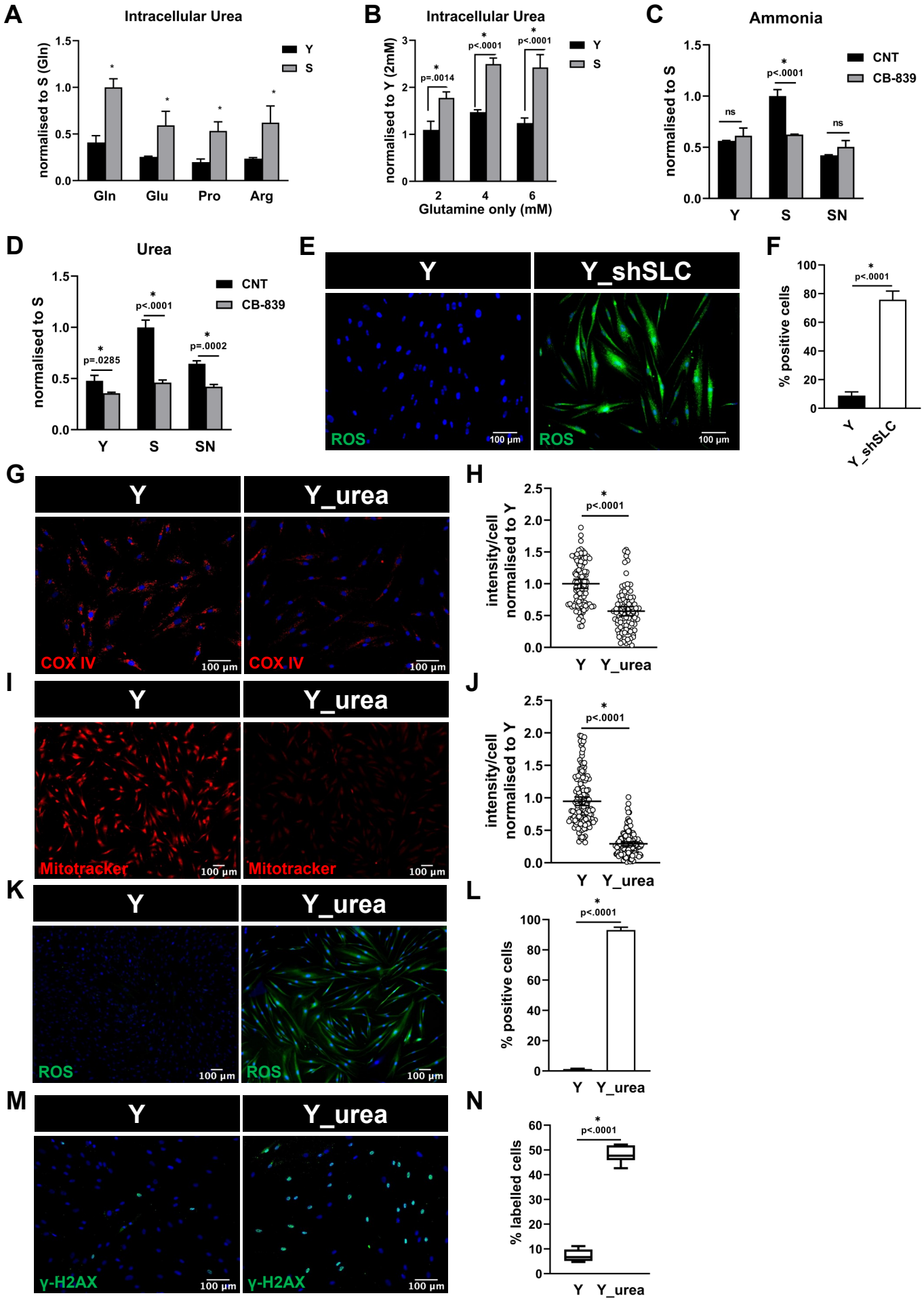
A
Intracellular Urea
normalised to S (Gln)
Y
S
Gln
Glu
Pro
Arg
B
Intracellular Urea
normalised to Y (2mM)
p=.0014
p<.0001
p<.0001
Glutamine only (mM)
C
Ammonia
normalised to S
CNT
CB-839
p<.0001
ns
Y
S
SN
D
Urea
normalised to S
p=.0285
p<.0001
p=.0002
E
Y
Y_shSLC
ROS
100 µm
F
% positive cells
p<.0001
G
Y
Y_urea
COX IV
H
intensity/cell normalised to Y
p<.0001
I
Mitotracker
J
K
L
% positive cells
p<.0001
M
γ-H2AX
N
% labelled cells
p<.0001

Figure S3. Glutamine contributes to urea accumulation in senescent cells, leading to manifestation of mitochondrial defect and aging hallmarks. Related to Figure 3.

(A) Intracellular urea measurement in Y and S cells after treatment with 2mM amino acids for 24hours; data normalised to S cells fed with glutamine; data shown as mean ± SD. * denotes $p < .05$ as compared to Y. (B) Intracellular urea measurement after cells were fed with different dosage of glutamine; data normalised to Y cells fed with 2mM glutamine; data shown as mean ± SD. **(**C) Intracellular Ammonia measurement in Y, S and SN cells with CB-839 treatment for 24hrs and without treatment (CNT); data normalised to S (CNT); data shown as mean ± SD. (D) Measurement of intracellular urea concentration with CB-839 treatment for 24hrs and without treatment (CNT); data normalised to S (CNT); data shown as mean ± SD. (E) Reactive oxygen species (ROS) was measured using DCFDA dye. (F) Quantification percentage of cells positive for ROS; data shown as mean ± SD, n>200 cells in 10 fields of view. (G-N) Y_urea denotes Y cells treated with 1 mM urea for 7days. (G) Immunostaining for COX IV, scale bar=100 μm; (H) Quantification of COX IV intensity per cell, normalised to Y; data shown as mean ± 95%CI for >100 cells. (I) Live stain images of Mitotracker Red, scale bar=100 μm. (J) Quantification of Mitotracker Red intensity per cell normalised to Y; data shown as mean ± 95%CI for >100 cells. (K) Live stain for ROS, using DCFDA dye, scale bar=100μm. (L) Quantification percentage of cells positive for ROS; data shown as mean ± SD, n>200 cells in 10 fields of view. (M) Immunostaining for γ-H2AX, a measure of DNA damage, scale bar=100μm. (N) Quantification percentage of cells positive for γ-H2AX; data shown as mean ± SD, n>200 cells in 10 fields of view.

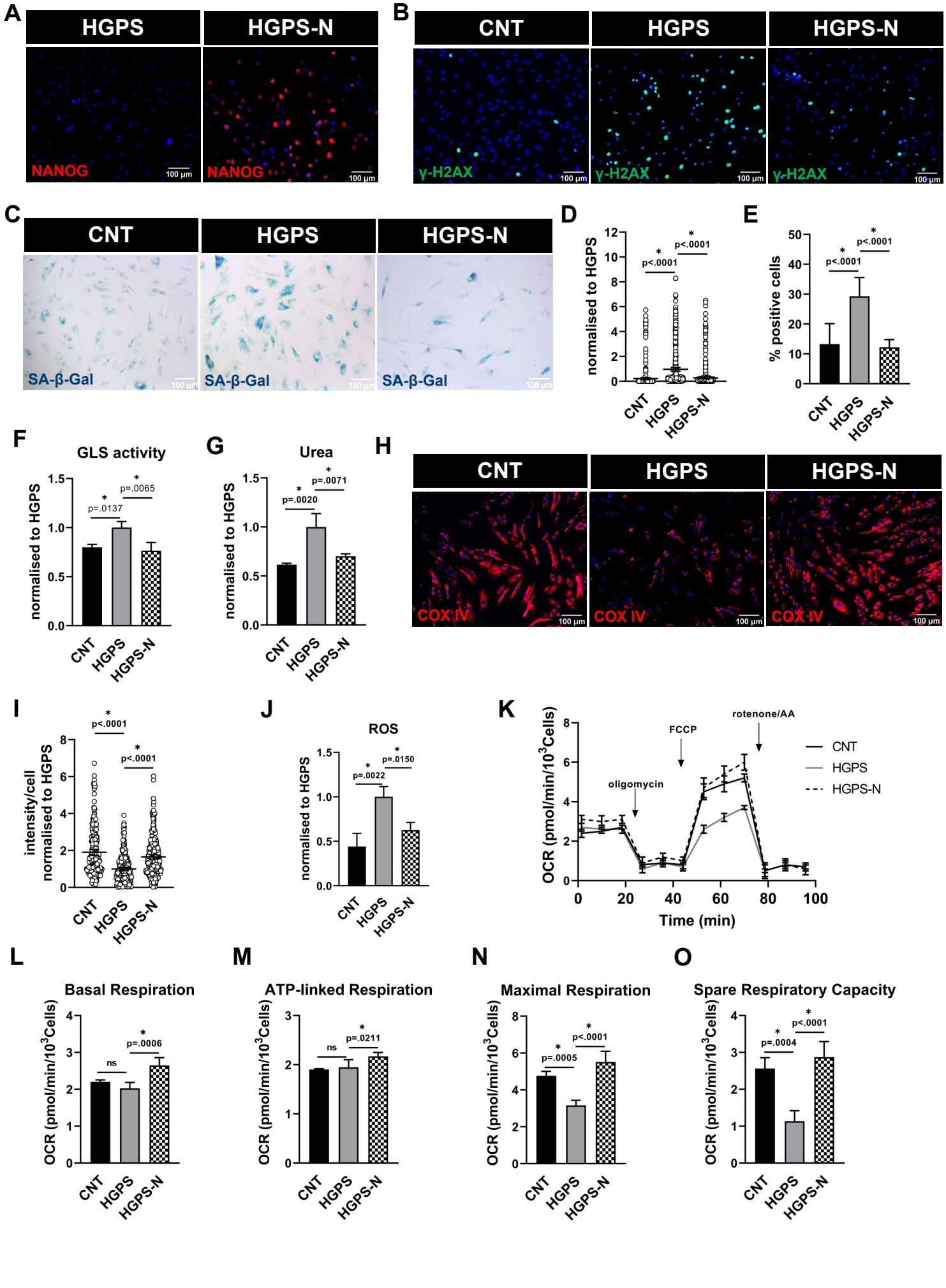
A
HGPS
HGPS-N
NANOG
NANOG
100 µm
100 µm
B
CNT
HGPS
HGPS-N
γ-H2AX
γ-H2AX
γ-H2AX
100 µm
C
CNT
HGPS
HGPS-N
SA-β-Gal
SA-β-Gal
SA-β-Gal
D
normalised to HGPS
p<.0001
p<.0001
CNT
HGPS
HGPS-N
E
% positive cells
p<.0001
p<.0001
F
GLS activity
normalised to HGPS
p=.0137
p=.0065
G
Urea
normalised to HGPS
p=.0020
p=.0071
H
COX IV
COX IV
COX IV
I
intensity/cell normalised to HGPS
p<.0001
p<.0001
J
ROS
normalised to HGPS
p=.0022
p=.0150
K
OCR (pmol/min/10³Cells)
oligomycin
FCCP
rotenone/AA
CNT
HGPS
HGPS-N
Time (min)
L
Basal Respiration
OCR (pmol/min/10³Cells)
ns
p=.0006
M
ATP-linked Respiration
OCR (pmol/min/10³Cells)
ns
p=.0211
N
Maximal Respiration
OCR (pmol/min/10³Cells)
p=.0005
p<.0001
O
Spare Respiratory Capacity
OCR (pmol/min/10³Cells)
p=.0004
p<.0001

Figure S4: Fibroblasts from progeria patients demonstrate aging hallmarks. Related to Figure 3.

(A) Immunostaining for NANOG expression and nuclear localization upon addition of DOX in the medium of NANOG transduced cells. Scale bar=100μm. (B) Immunostaining for γ-H2AX, scale bar=100μm. (C) Representative images of SA-β-gal staining in CNT, HGPS, HGPS-N cells. (D) Quantification of γ-H2AX intensity per cell, normalised to HGPS; data shown as mean ± 95%CI for >100 cells. (E) Percentage of senescent cells shown by SA-β-gal staining and quantification; data presented as mean ± SD, n = 3 independent experiments. (F) Measurement of glutaminase activity, data shown as mean ± SD. (G) Intracellular urea concentration, normalised to HGPS; data shown as mean ± SD. (H) Immunostaining for mitochondrial complex IV (COX IV), scale bar=100μm. (I) Quantification of COX IV intensity per cell. Data shown as mean ± 95%CI for >200 cells. (J) Measurement of ROS using DCFDA dye; data shown as mean ± SD. (K) Measurement of oxygen consumption (OCR) using Seahorse extracellular flux analyzer. (L-O) Basal Respiration (L), ATP-linked Respiration (M), Maximal Respiration (N) and Spare Respiratory Capacity (O) rates calculated from the OCR data in (K). Nomenclature: CNT= healthy fibroblasts from the father of the HGPS patient, HGPS= fibroblasts from patient with HGPS syndrome, HGPS-N= HGPS fibroblasts expressing NANOG upon Dox administration.

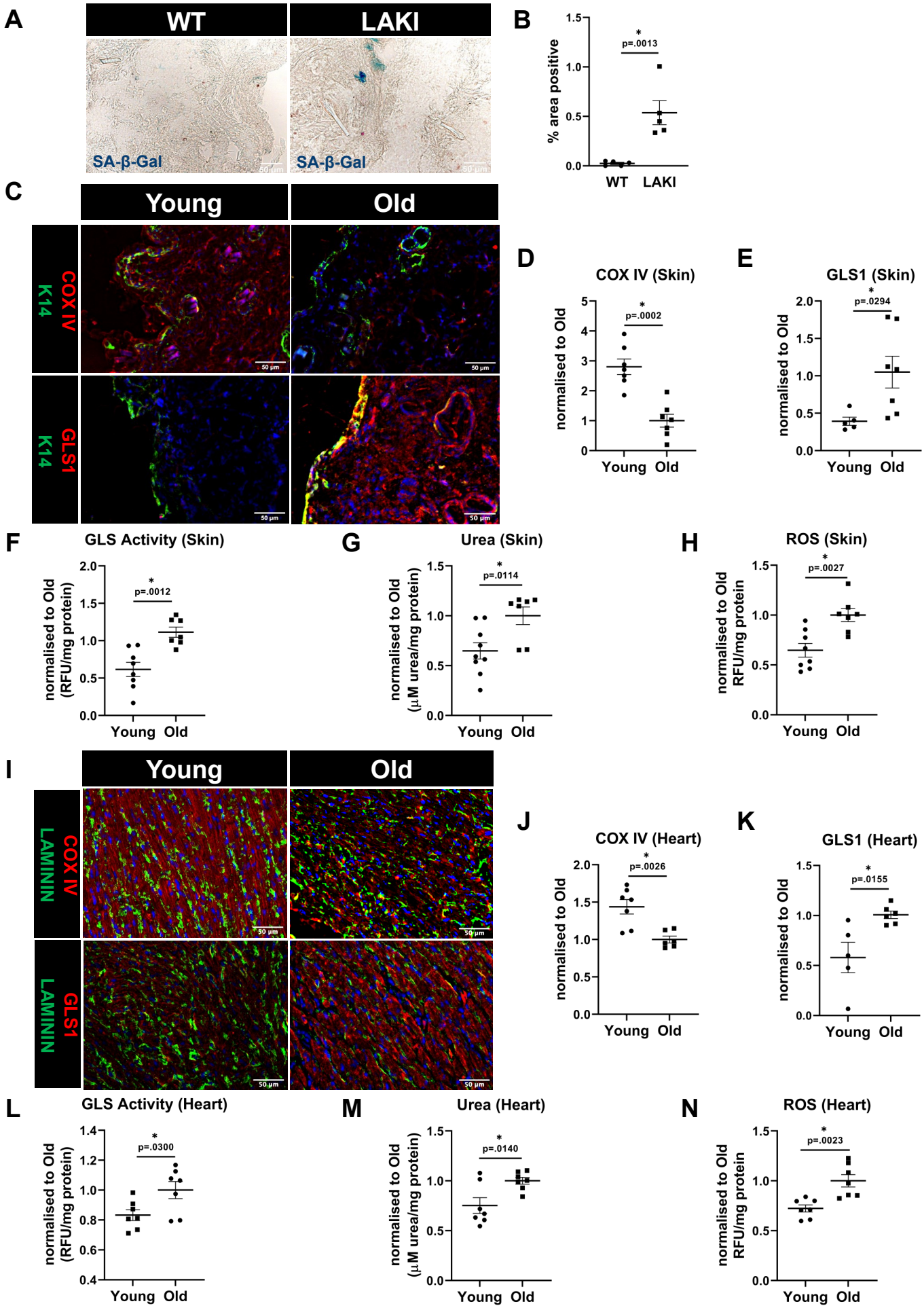
A
WT
LAKI
SA-β-Gal
SA-β-Gal
B
% area positive
p=.0013
WT
LAKI
C
Young
Old
COX IV
K14
GLS1
K14
D
COX IV (Skin)
normalised to Old
p=.0002
Young
Old
E
GLS1 (Skin)
normalised to Old
p=.0294
Young
Old
F
GLS Activity (Skin)
normalised to Old
(RFU/mg protein)
p=.0012
Young
Old
G
Urea (Skin)
normalised to Old
(µM urea/mg protein)
p=.0114
Young
Old
H
ROS (Skin)
normalised to Old
RFU/mg protein
p=.0027
Young
Old
I
Young
Old
COX IV
LAMININ
GLS1
LAMININ
J
COX IV (Heart)
normalised to Old
p=.0026
Young
Old
K
GLS1 (Heart)
normalised to Old
p=.0155
Young
Old
L
GLS Activity (Heart)
normalised to Old
(RFU/mg protein)
p=.0300
Young
Old
M
Urea (Heart)
normalised to Old
(µM urea/mg protein)
p=.0140
Young
Old
N
ROS (Heart)
normalised to Old
RFU/mg protein
p=.0023
Young
Old

Figure S5. Increasing urea production accompanied with less COX IV in aged mice. Related to Figure 4.

(A) SA-β-GAL staining and (B) quantification in skin of WT and heterozygous LAKI progeria mouse (LMNAG609G/+) at the age of 10 months. Representative immunostaining images and their quantification for COX IV and GLS1 in mouse skin (C-E) and heart tissue (I-K). GLS activity (F, L), Urea concentration (G, M) and ROS level (H, N) were evaluated in skin and heart of old and young mice. Young mice: 4-months-old mice; Old mice: 19-24 months old. Data shown as mean ± SE for each cohort of animals (each bubble represents a mouse, n=5-9). *: designates statistical significance as compared to LAKI with $p<0.05$.

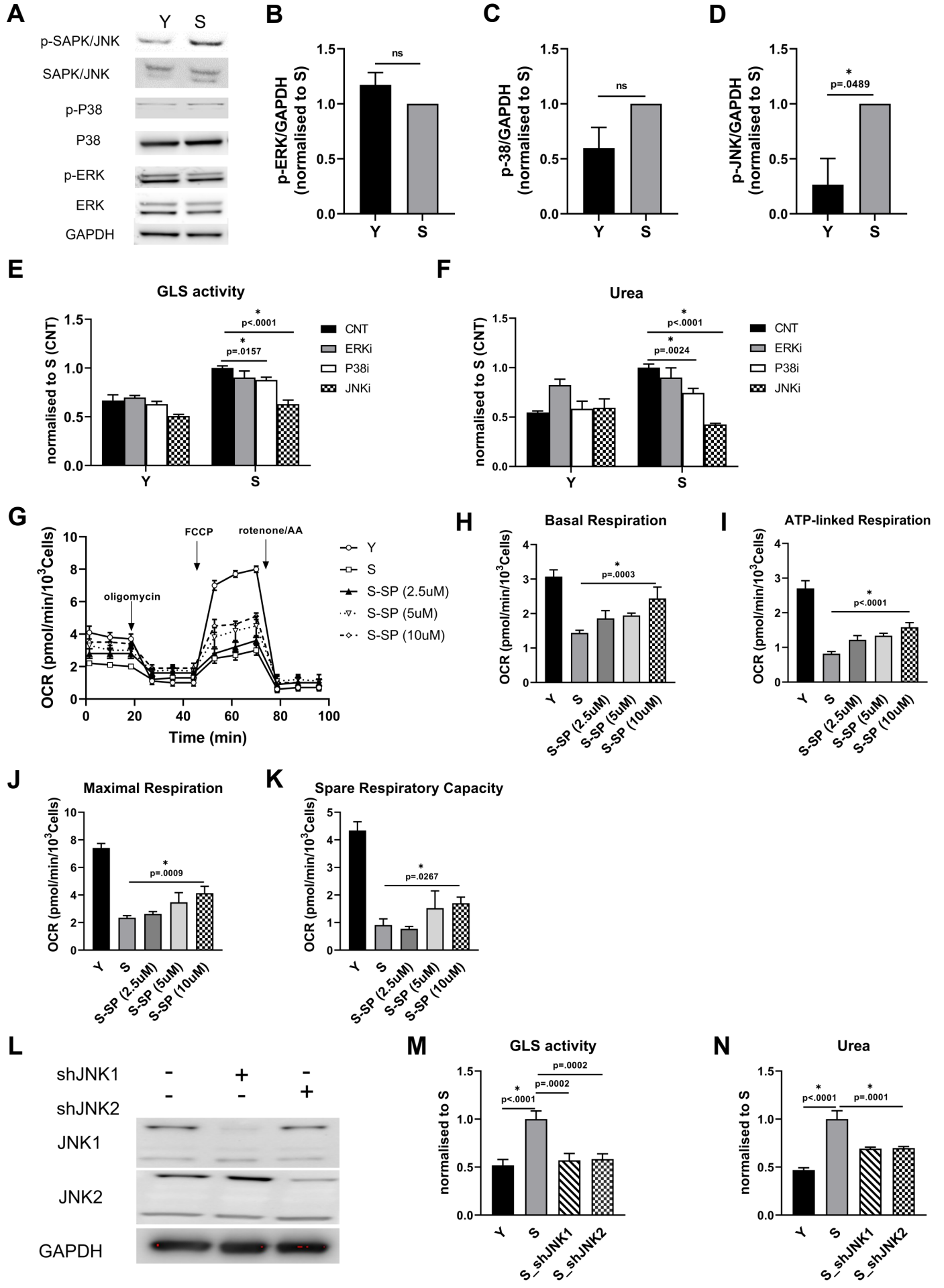
A
Y
S
p-SAPK/JNK
SAPK/JNK
p-P38
P38
p-ERK
ERK
GAPDH
B
p-ERK/GAPDH (normalised to S)
ns
C
p-38/GAPDH (normalised to S)
ns
D
p-JNK/GAPDH (normalised to S)
*
p=.0489
E
GLS activity
normalised to S (CNT)
*
p<.0001
*
p=.0157
CNT
ERKi
P38i
JNKi
F
Urea
normalised to S (CNT)
*
p<.0001
*
p=.0024
CNT
ERKi
P38i
JNKi
G
OCR (pmol/min/10^3Cells)
FCCP
rotenone/AA
oligomycin
Time (min)
Y
S
S-SP (2.5uM)
S-SP (5uM)
S-SP (10uM)
H
Basal Respiration
OCR (pmol/min/10^3Cells)
*
p=.0003
I
ATP-linked Respiration
OCR (pmol/min/10^3Cells)
*
p<.0001
J
Maximal Respiration
OCR (pmol/min/10^3Cells)
*
p=.0009
K
Spare Respiratory Capacity
OCR (pmol/min/10^3Cells)
*
p=.0267
L
shJNK1
shJNK2
JNK1
JNK2
GAPDH
M
GLS activity
normalised to S
p=.0002
p=.0002
*
p<.0001
S_shJNK1
S_shJNK2
N
Urea
normalised to S
*
p<.0001
*
p=.0001
S_shJNK1
S_shJNK2

Figure S6. JNK regulates glutaminase activity and mitochondrial function in senescent MSCs. Related to Figure 5.

(A-D) Western Blot analysis and quantification for the expression and phosphorylation of P38, ERK and JNK in Y and S cells show significant upregulation of p-JNK in S cells. GAPDH served as a loading control. Data normalised to S and represented as mean ± SD from 3 independent experiments. (E) Glutaminase activity and (F) urea concentration measurement with/without treatment of ERK, P38 and JNK inhibitors for 24 hrs. (G) Measurement of oxygen consumption (OCR) using Seahorse extracellular flux analyzer. S cells treated with SP600125 for 6 days (H-K) Calculations of Basal Respiration, ATP-linked Respiration, Maximal Respiration and Spare Respiratory Capacity rates based on OCR data. (L) Knockdown efficacy of JNK1 and JNK2 was characterized by Western blot analysis in senescent hf-MSC. (M) Glutaminase activity measurement in Y, S, JNK1 and JNK2 knockdown cells; data shown as mean ± SD. (N) Intracellular urea measurement, normalised to S; data shown as mean ± SD.

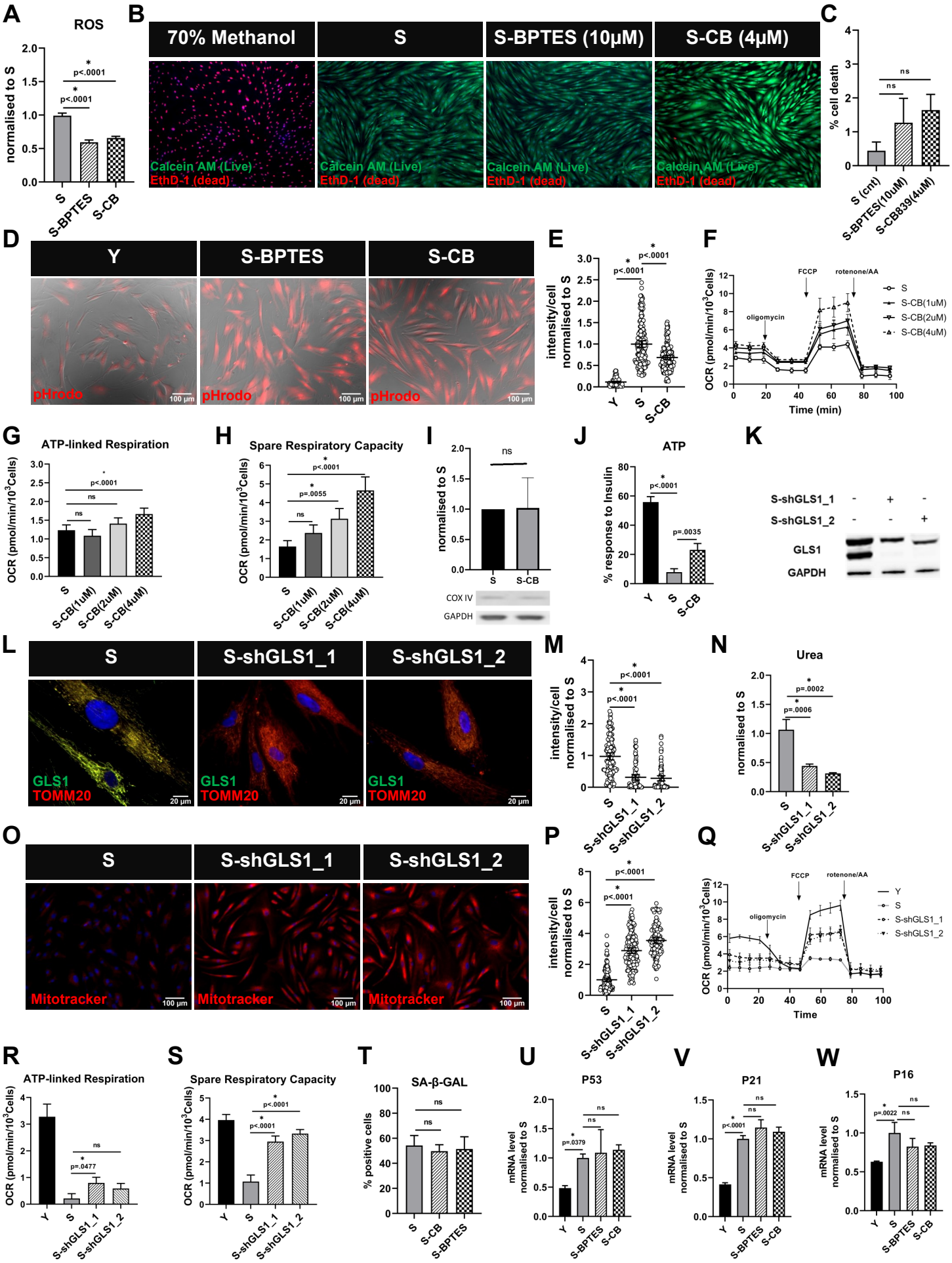
A
ROS
normalised to S
p<.0001
p<.0001
S
S-BPTES
S-CB
B
70% Methanol
S
S-BPTES (10μM)
S-CB (4μM)
Calcein AM (Live)
EthD-1 (dead)
C
% cell death
ns
ns
S (cnt)
S-BPTES(10uM)
S-CB839(4uM)
D
Y
S-BPTES
S-CB
pHrodo
100 μm
E
intensity/cell normalised to S
p<.0001
p<.0001
Y
S
S-CB
F
OCR (pmol/min/10³Cells)
FCCP
rotenone/AA
oligomycin
S
S-CB(1uM)
S-CB(2uM)
S-CB(4uM)
Time (min)
G
ATP-linked Respiration
OCR (pmol/min/10³Cells)
p<.0001
ns
ns
S
S-CB(1uM)
S-CB(2uM)
S-CB(4uM)
H
Spare Respiratory Capacity
OCR (pmol/min/10³Cells)
p<.0001
p=.0055
ns
S
S-CB(1uM)
S-CB(2uM)
S-CB(4uM)
I
normalised to S
ns
S
S-CB
COX IV
GAPDH
J
ATP
% response to Insulin
p<.0001
p=.0035
Y
S
S-CB
K
S-shGLS1_1
S-shGLS1_2
GLS1
GAPDH
L
S
S-shGLS1_1
S-shGLS1_2
GLS1
TOMM20
20 μm
M
intensity/cell normalised to S
p<.0001
p<.0001
S
S-shGLS1_1
S-shGLS1_2
N
Urea
normalised to S
p=.0002
p=.0006
S
S-shGLS1_1
S-shGLS1_2
O
S
S-shGLS1_1
S-shGLS1_2
Mitotracker
100 μm
P
intensity/cell normalised to S
p<.0001
p<.0001
S
S-shGLS1_1
S-shGLS1_2
Q
OCR (pmol/min/10³Cells)
FCCP
rotenone/AA
oligomycin
Y
S
S-shGLS1_1
S-shGLS1_2
Time
R
ATP-linked Respiration
OCR (pmol/min/10³Cells)
ns
p=.0477
Y
S
S-shGLS1_1
S-shGLS1_2
S
Spare Respiratory Capacity
OCR (pmol/min/10³Cells)
p<.0001
p<.0001
Y
S
S-shGLS1_1
S-shGLS1_2
T
SA-β-GAL
% positive cells
ns
ns
S
S-CB
S-BPTES
U
P53
mRNA level normalised to S
ns
ns
p=.0379
Y
S
S-BPTES
S-CB
V
P21
mRNA level normalised to S
ns
ns
p<.0001
Y
S
S-BPTES
S-CB
W
P16
mRNA level normalised to S
ns
ns
p=.0022
Y
S
S-BPTES
S-CB

Figure S7. Inhibition of GLS1 activity in senescent MSC restores mitochondrial function. Related to Figure 6.

(A) Measurement of ROS in S, S-BPTES and S-CB cells using DCFDA dye; data shown as mean ± SD. (B) Calcein AM (green, live cells) and ethidium homodimer (red, dead cells) staining of senescent MSCs, after treatment for 3 days with media containing GLS1 inhibitors. Methanol (70%) served as a positive control for non-viable cells, scale bar=200μM. (C) Quantification of percentage of cell viability; data shown as mean ± SD, n>200 cells, from 6 fields of view. (D) Measurement of intracellular pH using pHrodo Red AM intracellular pH indicator, scale bar=100 μM. (E) Quantification of pHrodo Red AM intensity per cell, normalised to S; data shown as mean ± 95%CI for >200 cells. (F) Measurement of oxygen consumption (OCR) using Seahorse extracellular flux analyzer of S cells after treatment with the indicated concentrations of GLS1 inhibitor, CB-839 for 10 days. (G) Calculations of ATP-linked respiration and (H) Spare Respiratory Capacity based on OCR data, demonstrating increased mitochondrial function after CB-839 treatment. (I) Western blot analysis for COX IV. (J) Intracellular ATP concentration measured in Y, S and S-CB (4μM) cells in response to insulin stimulation for 24 hours; data shown as mean ± SD. (K) WB for GLS1 of control cells or cells in which GLS1 was knocked down using the indicated shRNA. (L) Co-stain for GLS1 and TOMM20 (mitochondrial membrane protein) in senescent and GLS1 knocked down senescent cells, scale bar=20μM. (M) Quantification of GLS1 intensity, normalised to S cells, demonstrating efficient GLS1 knockdown; data shown as mean ± 95%CI for >100 cells. (N) Measurement of intracellular urea concentration normalised to S; represented as mean ± SD. (O) Representative images of Mitotracker Red live stain; scale bar=100μm. (P) Quantification of Mitotracker Red intensity per cell, normalised to S; data shown as mean ± 95%CI for >200 cells. (Q) Measurement of oxygen consumption rate (OCR) using Seahorse extracellular flux analyzer. (R) ATP-linked Respiration and (S) Spare Respiratory Capacity calculated from the OCR data in (Q); data shown as mean ± SD. (T) Percentage of senescent cells shown by SA-β-gal quantification; data presented as mean ± SD, n = 3 independent experiments. (U-W) Quantification of gene expression of cell cycle inhibitors *P53, P21 and P16* via quantitative PCR normalised to S and internally normalised to *RPL32* cycle number; data shown as mean ± SD.

Table S1. Primers used in real time PCR. Related to Star Methods

Human Gene	Forward (5'-3')	Reverse (3'-5')
GLUT1	TCTGGCATCAACGCTGTCTTC	CGATACCGGAGCCAATGGT
GLUT3	GCTGGGCATCGTTGTTGGA	GCACTTTGTAGGATAGCAGGAAG
GLUT4	ATCCTTGGACGATTCCTCATTGG	CAGGTGAGTGGGAGCAATCT
GLS1	CGAAGATTTGCTTTGTCAGCTATGG	CTCTGCAGCAGCTACATGGA
SLC14A1	GATTCTCCGGGGCATATCCC	CCAGGGGTTCTGAACAAGAAG
IL1α	CACGGCTGCTGCATTACATA	AGAGGAGGTTGGTCTCACTA
IL1β	GATGCACCTGTACGATCACT	ACGCAGGACAGGTACAGATT
IL6	GAGGAGACTTGCCTGGTGAA	TGGACTGCAGGAACTCCTTA
IL8	TTGGCAGCCTTCCTGATTTC	TCTTTAGCACTCCTTGGCAAAAC
P21	CCGCGACTGTGATGCGCTAA	TGCAGCAGAGCAGGTGAGGT
P53	GGCCATCTACAAGCAGTCAC	GGATGGTGGTACAGTCAGAG
P16	CTTCCTGGACACGCTGGT	GCATGGTTACTGCCTCTGGT

Table S2. Antibody dilution and application. Related to Star Methods

Antibody	Application	Dilution
Cytochrome C	ICC	1/200
COX IV	WB, ICC, IHC	1/1000, 1/200, 1/200
PDHA1 (phosphor S293)	ICC	1/200
KGA/GAC	WB, ICC, IHC	1/1000, 1/200, 1/200
Phospho-Histone H2A.X (Ser139)	ICC	1/200
Tomm20	ICC	1/200
Cytokeratin 14	IHC	1/100
Laminin	IHC	1/100
Goat anti-rabbit/anti-mouse IgG Secondary Antibidy	ICC, IHC	1/200
Hoechst 33342	ICC, IHC	1/200
p-SAPK/JNK	WB	1/1000
SAPK/JNK	WB	1/1000
p-P38	WB	1/1000
P38	WB	1/1000
p-ERK1/2	WB	1/1000
ERK1/2	WB	1/1000
JNK1	WB	1/500
JNK2	WB	1/1000(WB)
NANOG	ICC	1/1000
GAPDH	WB	1/10000
anti-rabbit IgG HRP linked	WB	1/1000(WB)
anti-mouse IgG HRP linked	WB	1/1000(WB)